Rail Surface Inspection System Using Differential Topographic Images

F. J. delaCalle*, Daniel F. García*, Rubén Usamentiaga*

*Department of Computer Science and Engineering, University of Oviedo, Campus de Viesques 33204 Gijón, Asturias, Spain, Email: delacalle@uniovi.es

***Abstract*—In this paper a surface inspection system for rails is presented. Rails must meet the strict requirements of international quality standards, however there are few commercial surface inspection systems for rails and also, a lack of publications describing the design and configuration of inspection systems in detail. Therefore, manufacturers must develop their own systems or buy one of the few commercial ones available. These systems also need a long, cumbersome and expensive configuration process the manufacturer cannot perform without the assistance of the inspection system provider. The system proposed in this paper needs a set of samples and the requirements of the international standards to carry out an automatic configuration process avoiding the cost of manual configuration. The system uses four profilometers to acquire the surface of the rail. The acquired data is compared to a mathematical model of the rail to generate differential topographic images of the surface of the rail. Then a computer vision algorithm is used to detect defects based on the tolerances established in the international quality standards. The system has been tested and validated using a set of rails and a rail pattern from ArcelorMittal, with better results than the other two systems installed in a factory [1].**

***Index Terms*—Long steel product, Rail inspection, Surface inspection, Defect detection, Computer vision**

I. Introduction

The steel industry needs high reliable quality control systems to control production. These systems must check the quality of the products to ensure they meet the strict requirements of the international standards in terms of surface quality, dimensions, flatness, etc.

Surface inspection is commonly carried out automatically by computer vision systems. These systems must give a diagnosis of each product to the manufacturer's quality inspectors. This diagnosis must contain the dimensions and location of every defect detected on the surface. Along with the defects detected, some erroneous detections are given to the quality inspectors. The inspectors must check every detection, so erroneous detections must be minimized. Due to current production speeds, the surface cannot be inspected manually: new reliable, fast and efficient inspection systems are needed.

Commercial surface inspection systems require a long, cumbersome and expensive configuration process that must be carried out by the engineers of the inspection system provider. Therefore, the manufacturers are unable to reconfigure their systems by themselves whenever they change their production line conditions. This configuration also needs the help of the manufacturer's quality inspectors in order to evaluate the system at every step.

This paper presents a new rail surface inspection system that is based directly on the requirements set in the international standards. The system produces differential topographic images of the surface of the rail in real-time to detect defects by applying the quality tolerances given in the standards. The processing procedure is automatically configurable by giving a set of samples and the requirements of the standards. This configuration addresses to the two most important metrics for the manufacturer: defect detection rate and the number of erroneous detections per product.

The system was tested using a set of produced rails from a real factory. The results have been compared with the performance of another two surface inspection systems, available in the same factory, improving the defect detection rate and also reducing the number of erroneous detections per product. The system has been validated using a rail pattern for surface inspection systems giving the same performance obtained in the tests.

The rest of the paper is organized as follows: In Section II a brief summary about related work is given. The proposed system is described in Section III while in Section IV the results of the system are discussed. Finally, the Section V concludes the paper.

II. Related Work

Surface inspection based on computer vision techniques is suitable for diverse kinds of materials and industries. Many papers study this kind of image processing algorithms and techniques, applying them to different fields [2][3][4]. These algorithms and techniques are frequently used in defect detection processes for metallic products [5] as well as in other fields such as fabric [6], phone screens [7] or food [8].

Surface inspection based on computer vision can be carried out applying different techniques. The most widely used techniques are the acquisition of 2D images and 3D reconstruction. In the case of long products there is another problem to solve, the whole surface of the product must be inspected so the product must be surrounded by sensors or cameras. This is the case of rails [9] or wood products [10]. This additional requirement makes the applications more complex because the

[1]This is an extended version of the paper presented in the 2020 IEEE Industry Applications Society Annual Meeting [1]

information acquired by all the sensors or cameras must be synchronized.

Some of these techniques make it possible to inspect the products not only in the production line, but also in their final placement. This is a great advantage in products, like rails [11] [12] or pipes [13], which must be inspected periodically for security reasons.

There are few commercial systems for surface inspection of long products, so the manufacturers are forced to develop their own systems or buy them from the few existing inspection system providers.

The most traditional surface inspection system uses one light source to illuminate the product to be inspected and acquire 2D traditional images. In the steel industry, these images are commonly grayscale images. Acquired images are processed in order to detect gray level variations that suggest the existence of a defect [14][15][7]. One of the most reliable commercial systems for surface inspection of steel is Parsytec by ISRA [16]. Parsytec uses this method to detect defects. Its detection method is based on the division of the image into small rectangles called tiles, which are processed by searching for anomalous values. In addition, the images that result from these techniques can be inspected by human operators to identify defects and other objects over the surface of the products. The main deficiency of these techniques is the lack of measurable information about the size of the detected defects or objects. Using this technique, volumetric defects such as protrusions or seams cannot be measured and a large number of false detections are introduced in the diagnosis due to color variations in the product surface or irregular illumination.

Photometric stereo techniques are 3D reconstruction techniques that use several cameras whose placement is well known. Using the information obtained from the cameras about the light reflected by the inspected product (from one or several light sources), it is possible to estimate the orientation of the surface [17]. To do so, the placement and the intensity of the light sources must be well known, which means these techniques are vulnerable to changing ambient light conditions. Using the obtained information, the surface of the product can be reconstructed. Depending on the number and position of the light sources, different techniques can be applied.

In the case of long products, one common approach is shape from shadow techniques, including the Spectral Image Differentiation Procedure [9]. Colored light sources are placed around the product to ensure that the defects will project a shadow over the surface in different directions corresponding to the different light sources. These techniques analyze the shadows produced on the surface in order to estimate the orientation and dimensions of defects. The shape of the surface of the product is then estimated based on on light intensity which can be affected by vibrations or natural light conditions [18]. Using the Spectral Image Differentiation Procedure a qualitative map of the scanned surface can be generated as images for further processing [19].

These photometric stereo techniques are very suitable for inspecting flat products such as steel strips [20] due to the ease of placing the different light sources. However, when the whole surface of long products must be inspected, this technique presents a problem with the positioning of the light sources in order to illuminate the entire surface homogeneously while generating the needed number of shadows.

Inspection systems using 3D laser scanning are suitable for many fields in industry as they provide a fast and accurate point cloud that represents the shape of the objects scanned [12]. The dense point clouds obtained with these systems have many types of applications. These kinds of systems use several pairs of laser sources and cameras surrounding the product to scan the whole surface [10]. These pairs of devices are usually sold as one pre-calibrated device called a profilometer.

In many cases, laser techniques are applied in the manufacturing industry to obtain a complete reconstruction of an object using robotic arms [21] or by taking cross sections of a piece while moving either the group of sensors or the piece [22]. In most cases the aim of these systems is to measure specific features of the products, such as volume [23] or roughness [24]. In the manufacturing industry, long products are scanned using these techniques in cross sections called profiles. From each profile a point cloud is obtained which can be used to measure dimensions [25] or flatness [26]. For this purpose, the point clouds are approximated by arcs and segments that can also be grouped for fitting planes or other kinds of surfaces.

Once the surface is scanned, the system must analyze it to detect defects on the surface. This analysis can be done using different approaches.

The first approach uses traditional image processing techniques to detect anomalies on the acquired images. This approach usually follows a traditional pipeline of operations that goes from a simple threshold to complex filters.

The second approach consists in neural networks used to process the image to detect defects by itself. This is conceptually the simplest option as it works as a single component that takes an image and gives a diagnosis.

The third approach is a hybrid one. The first part of the processing systems consist of a sequence of traditional operations that leads to proposed regions. In the last steps, a neural network is fed with these regions to classify them into defective or non-defective regions. This is the most useful, and the most commonly used approach, as it takes the best from both approaches [19]. The last steps can be done by several types of neural networks depending on the purpose: Convolutional Neural Networks (CNN) [27][28], Regional Neural Networks (R-CNN) [29] or Artificial Neural Networks (ANN or NN) [30].

III. Proposed System

In this paper the proposed system is tested and used on a production line of rails. Rails are a specific type of long product that must to fit International Standards in order to be used safely. These standards, like the EN13674-1[31], set quality requirements in several aspects. The tolerances with regard to surface quality are between 0.3 mm and 1 mm. This

means that any volumetric anomaly of more than 0.3 mm (in depth or height) from the desired shape is considered a defect. In the rest of the paper the products considered are rails, but the system can be applied to any product that can be defined by its cross section.

The proposed system is composed of two subsystems working together to give a diagnosis of the quality of the surface in real-time. The first subsystem controls the sensors around the product. This system gets the data from the sensors and produces a composed image representing the deviations from the desired surface as gray values. The acquisition is triggered by an encoder signal sent from the production line. This subsystem is located in the Acquisition Computer. It uses 3D laser scanning technology to do so. This system has four profilometers placed around the path of the product that must be inspected. While the product moves under the sensors they are triggered to scan the surface and send the data to the system. The second subsystem gets the images from the previous one and analyzes them to detect defects on the product surface. This subsystem is located in the Master Computer.

The two subsystems are located in two different computers but they must communicate with each other and with the central control of the factory. This is carried out using two technologies. The communication with the rest of the systems of the factory is done using simple TCP messages that give the information about the product model and the international standard that must be met. The communication between the subsystems is performed using RabbitMQ, an implementation of the standard protocol AMQP. Therefore, if another system needs information about the product being inspected it only needs to join the appropriate message queue.

The computer in which the processing algorithm is located is also used as a storage computer and viewer. A complete view of the system and its components is shown in Figure 1.

A. Image Acquisition System

The acquisition of the raw data is carried out by four profilometers placed around the product. These sensors are Gocators 2350 by LMI. They are placed on two laser planes so they do not produce interferences between them. Therefore, as they are placed in pairs, the data of two of them must be rotated to be merged with the data given by the others.

While the product is moving, the profilometers acquire profiles of the product triggered by an encoder signal. The encoder signal is sent to the Profilometer Controller that is in charge of synchronizing the reception of the encoder signal to the four sensors. This ensures that a trigger signal is received by the four sensors at the same time, allowing the matching between them. The acquisition starts when the subsystem receives the start signal sent by the Master Computer.

The two laser planes are between two photocells. These photocells detect when the product enters in the measurement zone and when it leaves it. The pressence signal is sent to the Master Computer by the pair of photocells when either one of them detects a rail. Therefore, the systems starts acquiring profiles before the rail goes through the first laser plane and stop acquiring after the rail has passed the second laser plane. This produces a set of empty profiles at the beggining and at the end of the rail which is usefull for the inspectors to see if the rail has been acquired completly.

The full profile of the product is composed of the profiles given by the four profilometers. These profiles are point clouds that represent the surface of the product. In their raw format these profiles cannot be merged, a transformation is needed to make them all fit into the same coordinate system.

The point clouds are aligned to the mathematical shape of the product. The mathematical shape is called a model, which is a set of arcs and segments that perfectly defines the shape that the product should have. This aligning method is called registration. In order to perform the registration of the four acquired point clouds, four different partial-models are defined. A partial-model is defined as the part of the model that can be acquired by one of the profilometers.

The registration is performed in two steps. First a coarse registration is performed to align the clouds and the models by aligning their centroid and their orientation. In this case the orientation is computed using PCA (Principal Component Analysis). Once this first step is performed, a second step of registration is needed. The second step is an iterative registration procedure using the ICP (Iterative Closest Point) algorithm. Figure 2 shows the four raw profiles acquired by the profilometers and the result of the registration procedure.

After aligning the point clouds, the distances between the cloud and the model are calculated to obtain the deviations. These deviations are represented along the surface of the product as a flat representation. With this information an image is generated composed of a set of profiles representing a differential topographic image of the surface of the product along its longitudinal axis.

A profile is acquired every time the profilometer receives the trigger signal from the controller. The encoder from the production line works at a frequency of 500 Hz and the product moves at 1 m/s, so the profilometers acquire scans of the surface of the product every 2 mm. The acquisition frequency sets the real-time constraints for the acquisition procedure at 2 ms per profile.

Whereas the resolution of the sensor could be cappable of acquiring enough points to represent the whole surface of a product, there are some areas that are acquired non perpendicular which generates a lack of measurements. The lack of points in some areas can cause noise in the resulting image producing errors in the detection process. This noise is shown in Figure 3 where a dimensional defect is shown in red with many gaps between the measurements due to these oblique zones.

This lack of points is solved in the propossed system using a linear approach in those areas. Where an empty slot in the profiles is detected, the nearest points are used to linearly interpolate a new point in the empty slot. This is performed only if the distance between the nearest points is less than 10 millimeters (40 empty slots). In case there are many

This article has been accepted for publication in a future issue of this journal, but has not been fully edited. Content may change prior to final publication. Citation information: DOI 10.1109/TIA.2021.3059605, IEEE Transactions on Industry Applications

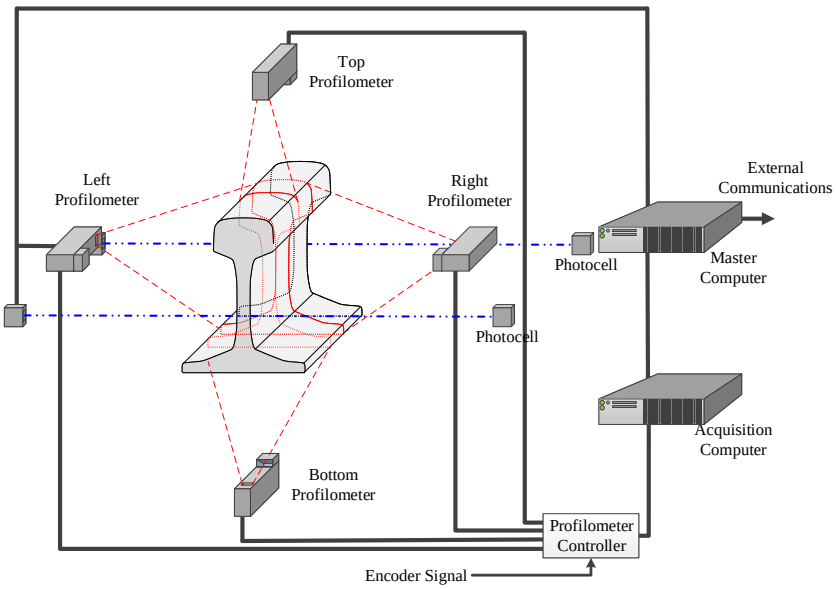

(a) General architecture

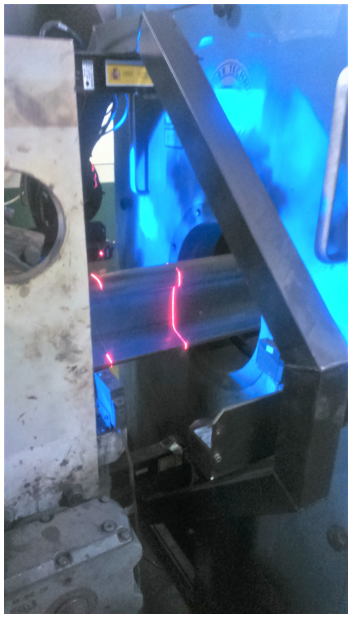

(b) System installed

Fig. 1: System Overview.

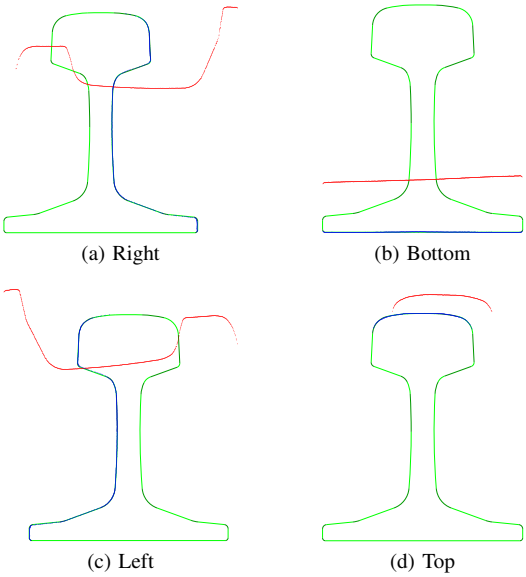

(a) Right (b) Bottom

(c) Left (d) Top

Fig. 2: Registration of the point clouds. Original data in red, model in green and result in blue

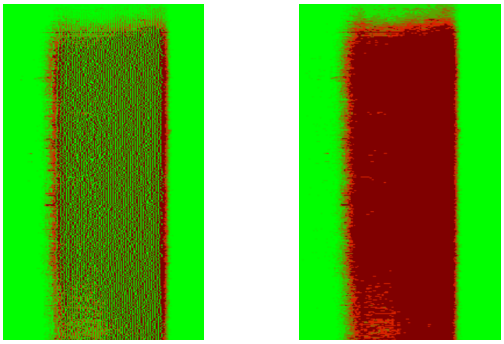

(a) Without interpolation (b) With interpolation

Fig. 3: Noise produced by empty slots in the image.

consecutive empty slots, the interpolation would not give a good representation of the shape of the product so they are set as 0-value pixels in order to be discarded while processing the image. Being x the position in the perimeter of the product and y the deviation from the perfect shape of a point p and the nearest points $p_1 = (x_1, y_1)$ and $p_2 = (x_2, y_2)$, the definition of the propossed method is divided into four alternatives: if the gap is too long (1), if the gap is not too long and located at the beginning of the image (2), if the gap is not too long and located at the end of the image (3) and if the gap is not too long and both p_1 and p_2 exist (4).

This procedure about filling the gaps is shown in Figure 4. This figure shows one of these areas that produces lack of points due to the position of the sensors (which is placed to get the maximum area of the product perpendiculary). This zone is the bottom of the head of the rails, in which it can be seen that the number of points is far less than in other zones. As the contour is divided in slots of 0.25 millimeters, there are several empty slots that are filled using linear interpolation (red crosses) betweenthe nearest points (white crosses).

$$y = 0; \forall x : (x_2 - x_1) > 10 \tag{1}$$

$$y = y_2; \forall p : \nexists p_1 \wedge (x_2 - x) \leq 10 \tag{2}$$

This article has been accepted for publication in a future issue of this journal, but has not been fully edited. Content may change prior to final publication. Citation information: DOI 10.1109/TIA.2021.3059605, IEEE Transactions on Industry Applications

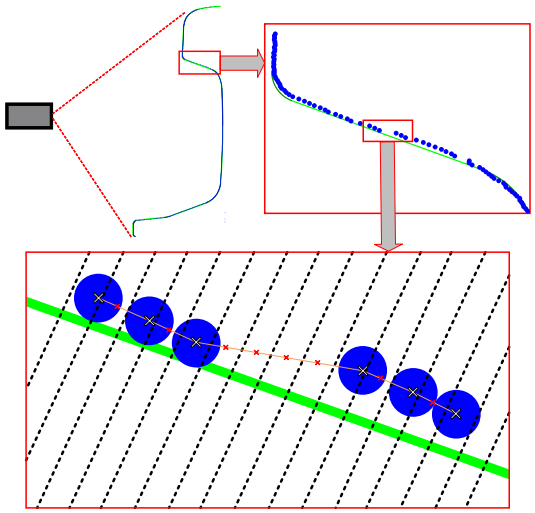

Fig. 4: Filling the gaps in the acquired profiles

Intel Core I7 3.60 GHz 16GB RAM			
Metric	Mean	Percent 95	Percent 99
Registration time (ms)	0.137	0.271	0.709
Differential map calculation time (ms)	0.391	0.559	1.087
Total process time (ms)	0.591	1.025	1.528
Mean Distance model to cloud (mm)	0.140	0.143	0.144
Intel Xeon E5 3.00 GHz 32GB RAM			
Metric	Mean	Percent 95	Percent 99
Registration time (ms)	0.142	0.276	0.780
Differential map calculation time (ms)	0.378	0.614	1.094
Total process time (ms)	0.590	1.016	1.625
Mean Distance model to cloud (mm)	0.140	0.142	0.144

TABLE I: Acquisition procedure measurements per profile

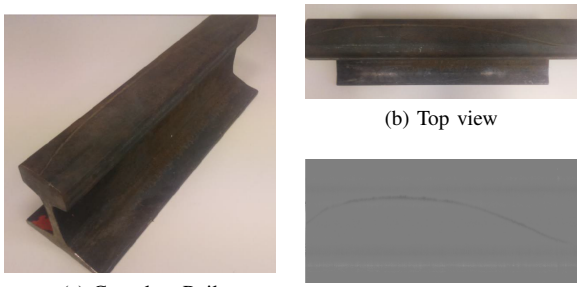

(a) Complete Rail

(b) Top view

(c) Resulting image

Fig. 5: Example A

$$y = y_1; \forall p : \nexists p_2 \wedge (x - x_1) \leq 10 \tag{3}$$

$$y = y = \frac{(x - x_1) \cdot (y_2 - y_1)}{(x_2 - x_1)} + y_1; \quad \forall p : \exists p_1, p_2 \wedge (x_2 - x_1) \leq 10 \tag{4}$$

Exhaustive tests have been done to verify that the acquisition system can work in real-time conditions. These tests were performed on 50 rails, 110 meters in length, producing measurements of 2,750,000 profiles. The acquisition procedure was tested on two platforms proving that 99 percent of the instances meet the real-time constraints (see Table I). These tests and detailed explanation of the acquisition procedure from the raw point clouds to the final format of the images are explained in [32].

Two examples of the final images are shown in Figure 5 and Figure 6. In these images, two surface defects can be seen: in Example A there is a lash produced by the straightening machine while in Example B there is a rolled-in material on the head of the rail. These defects caused these rails to be rejected by the production line and not sold.

B. Image Processing System

The processing subsystem is allocated in the Master Computer. The procedure used for processing the images is based on a traditional computer vision pipeline. This procedure, based on the images themselves, uses the tolerances set in the international standards, such as EN13674-1[31] in Europe. A detailed description of the processing algorithm as well as a configuration procedure is published in [33].

The generated images show some defects that are not surface defects. Dimensional defects can appear as a continuous defect in the images because of the comparison of the point clouds against the model. That is why the first step of the processing procedure is a filter. The aim of this filter is to remove the dimensional defects from the images in order to maintain only the surface defects. In order to to so, the median filter computes the median of a rectangle arround each pixel and subtracted that value from the pixel.

The size of the rectangle used in the filter must be enough to filter dimensional defects but maintaining the surface defects. In this system the dimensions of this rectangle are set as they fit the third part of the height of the image in length and 1 pixel in width. This erases dimensional defects but not the intrinsic noise produced by the profilometers or the defects.

According to the image generation method, some parts of the image may remain with exact 0 value due to occlusions or oblique acquisitions. These zones must be detected and eliminated from the ROI(Region Of Interest). As the gaps in the image can vary from profile to profile in the oblique zones, they must be located and put together in order to not process those areas. To do so a threshold is performed from the values 0 to 0 to detectd only exact 0 values. These thresholded zones are then dilated in order to eliminate as rolled product in their surroundings. As rolled product is a surface anomaly that appears at the start and end of a rolled product, it is not considered a defect because these part of the products is usually cut off before selling.

This article has been accepted for publication in a future issue of this journal, but has not been fully edited. Content may change prior to final publication. Citation information: DOI 10.1109/TIA.2021.3059605, IEEE Transactions on Industry Applications

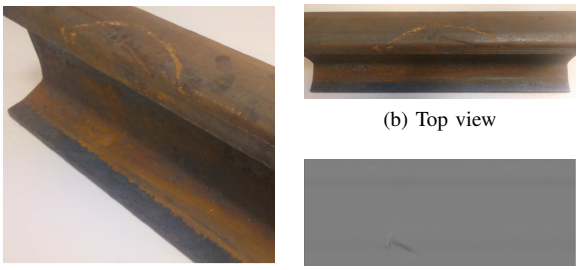

(a) Complete Rail (b) Top view (c) Resulting image

Fig. 6: Example B

Using the method explained above, the start and the end of the rail is also located and eliminated from the detection process. Due to the position of both starting and ending photocell, there is a part in the starting and ending image which does not contains data. These zones are also dilated in the longitudinal axis in order to eliminate them.

As the images have a direct translation to real world dimensions, they can be directly compared with the international standards. Therefore, the second step of the processing procedure is a thresholding based on the tolerances of the international standards. This thresholding detects any volumetric anomaly that differs from the perfect shape when the deviation is greater than the value defined by the standards. In the case of rails, the strictest tolerance is 0.3 millimeters for the head of the rails. This means that any anomaly that differs more than 0.3 millimeters from the perfect shape is classed as a defect. However, the tolerance defined by the standards sets a different threshold for each part of the rail.

After thresholding, two morphological operations are performed over the detected regions: an opening and a closing. An opening is the erosion of the regions followed by a dilation which reduces detected noise by eliminating small regions. Closing is the opposite, a dilation followed by an erosion, which joins the regions that are near.

Once the segmentation is finished, the resulting regions are evaluated in order to filter the erroneous detections, which can be scales, identification labels, etc. This filtering is performed in two steps. The first one is a filter based on the Bayesian Decision Theory [34]. The environment of the detected regions is studied in order to check if they differ from their environment. If the region is similar to its environment, it may be because the detection of that region is erroneous because of scales or dirt. This similarity is calculated in this procedure as the percentage of out-of-the-threshold pixels in the environment.

The last step of the procedure is a neural filter based on a multilayer perceptron. In order to train the network, 44 features are obtained from each region. These features are divided in two sets [35]. The first set of features is based on the morphology of the region. This set contains 14 features, including: length and width, center of the rectangular bounding box, convexity, compactness, etc. This set gives information about the location and shape of the defect. The second set contains 30 features that use the information about the gray level of the region. Features of this set give information about the appearance of the defect such as its mean value, and also information about how the values are located using features such as correlation, gravity center or homogeneity.

The whole procedure can be automatically configured using a set of samples. This differs from commercial systems, which must be configured manually by engineers of the inspection system provider in collaboration with the quality engineers of the manufacturer company. This is usually a long, cumbersome and expensive process that can be avoided using an automatic configuration.

C. Communication and visualization

All the communications in the system are carried out by message queues using RabbitMQ, an implementation of the standard protocol AMQP. The RabbitMQ server runs on the Master Computer, so the rest of the systems of the factory can also subscribe to the queue in order to get information of the system and the diagnosis it gives. A scheme of the whole communication system can be seen in Figure 7.

There are several forms of communications in the system. The communications with the sensors and the photocell that signals the presence of a rail is carried out by the driver of each device using a TCP connection. The communication with the rest of the systems of the factory is carried out by the Management and Visualization Module (MVM), shown in Figure 8, using a direct TCP connection.

The communications between the different modules of the system are performed using message queues. For instance, the normal work-flow for a rail should be as follows. First, the model of the rail, its identification number and the international standard it must meet is sent by the Factory Control to the Master Computer. When the photocell is activated, the Management and Visualization Module (MVM) posts a message in the queue Control.StartProduct. The Acquisition Subsystem is subscribed to Control.# so it gets the message from Control.StartProduct and it starts the acquisition until it gets another one from Control.EndProduct. While the rail is being inspected, the Acquisition Subsystem posts the generated images in Results.Images and the Processing Subsystem takes them from that queue. The Processing Subsystem processes the images and stores the information while it also posts it in Results.Defects from which the MVM obtains and shows it.

An important part of the system is the MVM. This is the module used by quality inspectors to check the defects in the rails. The random noise in the images should be eliminated to give a smooth surface where the defects can be easily observed. The intrinsic noise from the acquisition with the profilometers is measured on a completely flat surface. The noise in this experiment is approximately between -0.1 and 0.1 millimeters (see Figure 9). In order to give a useful diagnosis, the images are also colored depending on the international standard that is being used. The application offers three different views of the same image, as seen in Figure 10, using

This article has been accepted for publication in a future issue of this journal, but has not been fully edited. Content may change prior to final publication. Citation information: DOI 10.1109/TIA.2021.3059605, IEEE Transactions on Industry Applications

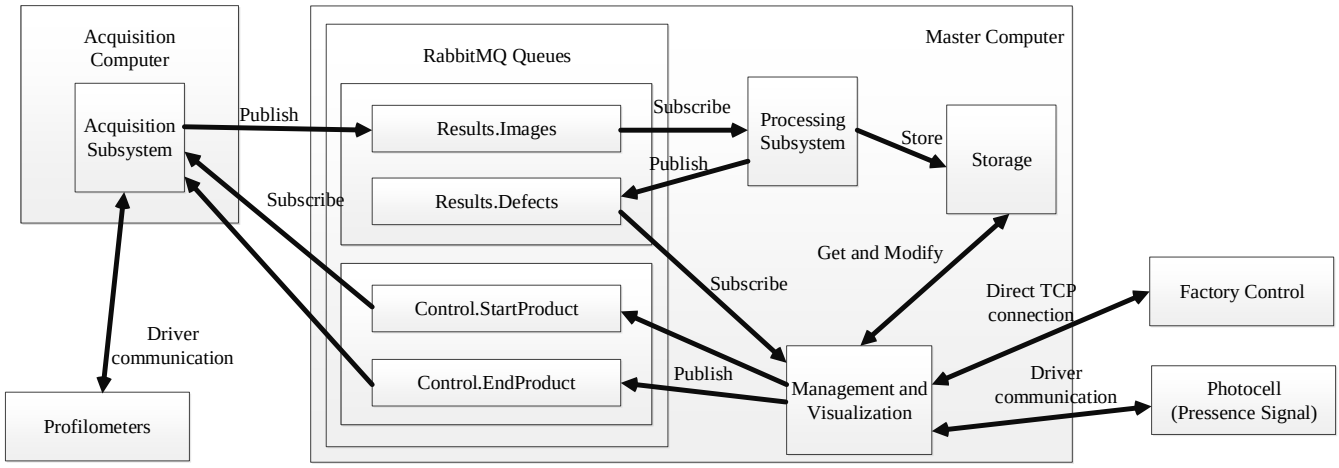

Fig. 7: System Communications

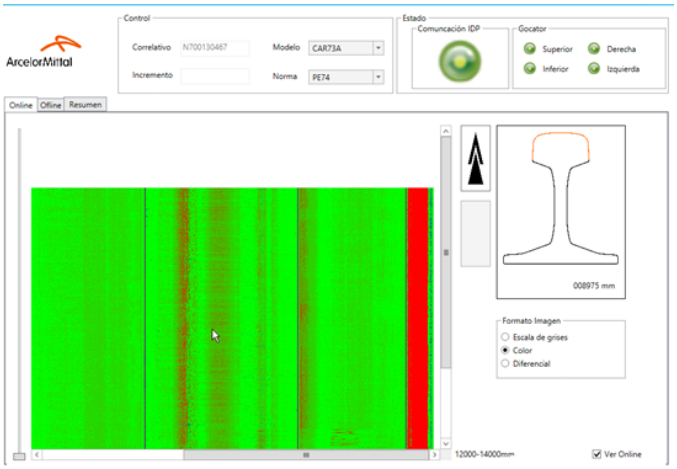

Fig. 8: Management and visualization interface

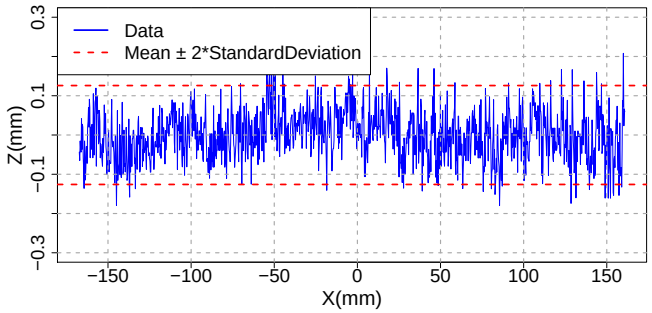

Fig. 9: Acquisition of a perfectly flat surface with a profilometer to test the noise of the sensor

Example A from Figure 5, where everything that surpasses one of the tolerances is shown in a different color.

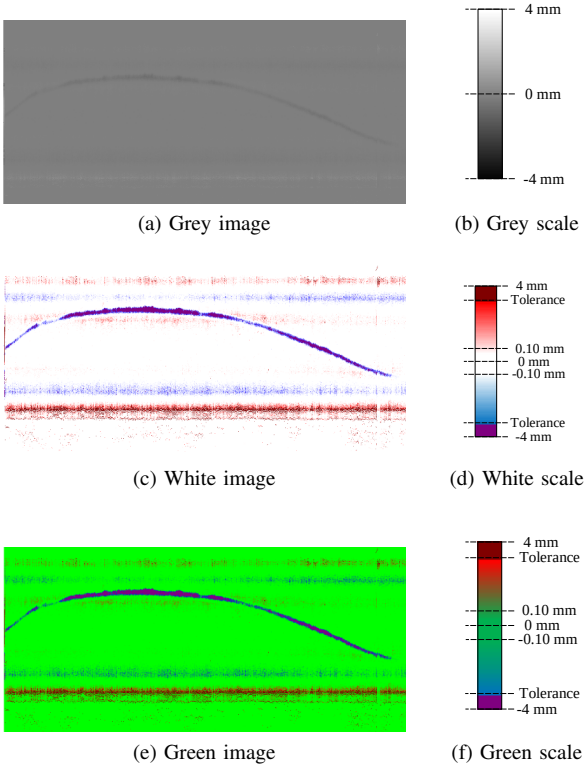

(a) Grey image (b) Grey scale

(c) White image (d) White scale

(e) Green image (f) Green scale

Fig. 10: Different views of the images

IV. Results

The proposed system was tested and validated. In order to do so, the diagnosis given by the system was compared with a manual diagnosis carried out by quality inspectors of ArcelorMittal, where the system is installed. This manual diagnosis of a set of rails is called Ground Truth. In this set, everything labeled by the inspectors must be recognized as a

This article has been accepted for publication in a future issue of this journal, but has not been fully edited. Content may change prior to final publication. Citation information: DOI 10.1109/TIA.2021.3059605, IEEE Transactions on Industry Applications

Metric	Proposed System	Proposed System Before NN	System A	System B
Recall	0.63	0.82	0.37	0.46
FP per Rail	6	38	27	8

TABLE II: Result comparison

defect whereas any other detected anomaly must be considered as an erroneous detection.

The proposed system was also compared with two other surface inspection systems. These other systems use stereo photogrametry in order to perform the inspection. These systems are labeled as A and B where A is a commercial system that uses a procedure described in [9] and B is an open system developed in [19].

The system must also be validated. A surface inspection rail pattern is used in order to check if the defects on the pattern are detected or not.

A. Ground Truth

The Ground Truth must include enough samples to represent the production of the manufacturer. In this case, the production was represented by 50 images of each of 65 inspected rails with at least one defect. The Ground Truth has 105 defects in total, 55 identification stickers as well as abundant dirt and scales. The comparison of the diagnosis of the system about the Ground Truth is performed in such a way that everything that does not intersect with something in the Ground Truth is a False Positive. In the same way, any labeled region in the Ground Truth that intersects with the diagnosis is treated as a True Positive, whereas everything that does not is treated as a False Negative.

After performing the comparison of each diagnosis, several values can be obtained: number of True Positives (TP), number of False Positives (FP) and number of False Negatives (FN). Using these values two useful metrics for the rail manufacturing industry can be calculated: Recall and FP per product. Recall, calculated in (5), is the percentage of defects detected by the system. The number of FP per rail is a very useful metric because every defective rail must be inspected manually in order to check if it can be repaired or not. Thus, any erroneous detection should be checked with the consequent cost in time for the quality inspectors. Therefore, the aim of the rail manufacturer will always be to have the highest possible Recall with the fewest possible FP per rail.

$$Recall = \frac{TP}{TP + FN} \tag{5}$$

The results of the comparison are shown in Table II. These results show that the proposed system has better results than the two other systems evaluated. An example of two defects detected by the system is shown in the Figure 11 along with the same defect captured by one of the photogrametric systems.

B. Validation Rail Pattern

The system was validated using a rail pattern for surface inspection systems. This pattern has several marks made by hand. These marks go from 0.4 to 0.9 millimeters in depth, 0.25 to 0.75 millimeters in width and 8 to 30 millimeters in length.

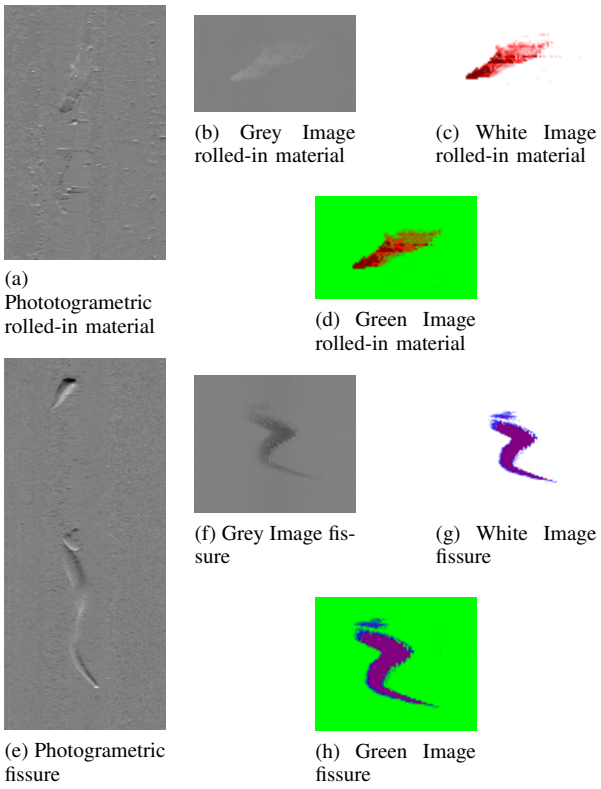

(a) Phototogrametric rolled-in material

(b) Grey Image rolled-in material

(c) White Image rolled-in material

(d) Green Image rolled-in material

(e) Photogrametric fissure

(f) Grey Image fissure

(g) White Image fissure

(h) Green Image fissure

Fig. 11: Result examples of a rolled-in material and a fissure.

The system was tested twice using this pattern. In order to give a detailed result, the diagnosis is separated in two sections: before and after the neural network filtering. The results are shown in Table III. The new system is capable of detecting all the defects except the one of 0.25 millimeters width, which is near the resolution of the profilometers. Performing the neural filtering, some defects are missed in order to erase erroneous detections, but 60% of the defects are maintained. After the filtering, only 8 erroneous detections are left but all of them are at the beginning and ending of the rail, which are zones that are usually cut and not sold. The proposed system gives better results than the other two system evaluated reducing the number of erroneous detections per rail and also increasing the defect detection rate, even after the neural filter. Two of these detected defects can be seen in Figure 12b.

The rail pattern used has also a big dimensional defect on it that the system can handle and elimate. Figure 12a shows the first image of the rail pattern with the dimensional defect on it and the same image after the processing, which includes noise reduction, surface defect detection and dimensional defect elimination.

The rail pattern also includes some well known engravings that can be measured in order to evaluate the precission of the system when measuring surface anomalies. This marks

This article has been accepted for publication in a future issue of this journal, but has not been fully edited. Content may change prior to final publication. Citation information: DOI 10.1109/TIA.2021.3059605, IEEE Transactions on Industry Applications

Number	Depth	Width	Length	Before NN	After NN
1	0.7 mm	0.5 mm	30 mm	X	-
2	0.8 mm	0.5 mm	30 mm	X	-
3	0.8 mm	0.75 mm	20 mm	X	X
4	0.9 mm	0.5 mm	20 mm	X	X
5	0.5 mm	0.5 mm	30 mm	X	X
6	0.5 mm	0.5 mm	30 mm	X	X
7	0.7 mm	0.5 mm	16 mm	X	X
8	0.5 mm	0.5 mm	20 mm	X	-
9	0.7 mm	0.5 mm	8 mm	X	X
10	0.8 mm	0.25 mm	16 mm	-	-
11	0.4 mm	0.75 mm	18 mm	X	X

TABLE III: Defects in the rail pattern

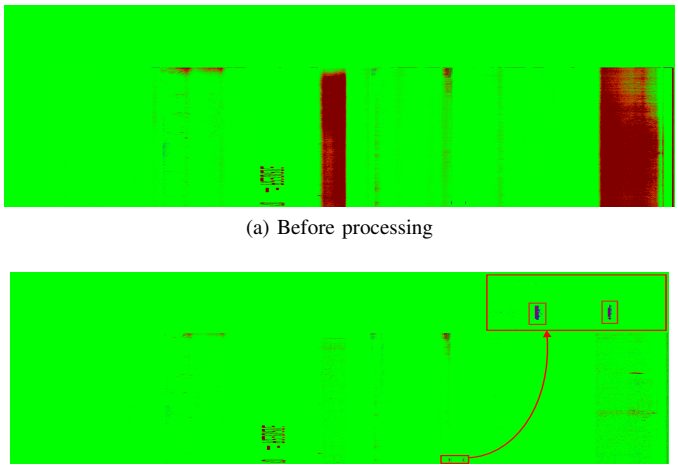

(a) Before processing

(b) After processing

Fig. 12: Rail pattern result example.

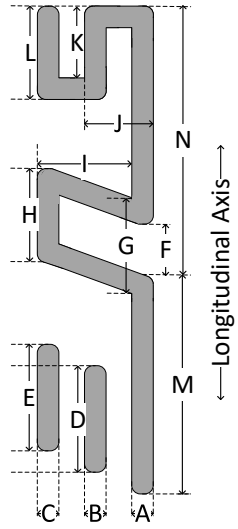

Fig. 13: Dimension measurements in Rail Pattern

Dimension	Real	Acquired	Difference	Axis
A	3.36 mm	3.25 mm	0.11 mm	Transversal
B	3.20 mm	3.00 mm	0.20 mm	Transversal
C	3.20 mm	3.00 mm	0.20 mm	Transversal
D	14.00 mm	14.00 mm	0.00 mm	Longitudinal
E	14.00 mm	12.00 mm	2.00 mm	Longitudinal
F	11.00 mm	10.00 mm	1.00 mm	Longitudinal
G	18.00 mm	20.00 mm	2.00 mm	Longitudinal
H	16.30 mm	16.00 mm	0.30 mm	Longitudinal
I	24.15 mm	24.00 mm	0.15 mm	Transversal
J	14.50 mm	14.25 mm	0.25 mm	Transversal
K	13.60 mm	14.00 mm	0.40 mm	Longitudinal
L	16.12 mm	16.00 mm	0.12 mm	Longitudinal
M	26.00 mm	26.00 mm	0.00 mm	Longitudinal
N	28.55 mm	28.00 mm	0.55 mm	Longitudinal
Height	1.15 mm	1.17 mm	0.02 mm	Z-Axis

TABLE IV: Results of dimension measurements in Rail Pattern

are protrusions on one side of the rail. The measurements are performed in both directions, transversal and longitudinal even when the dimensions of the pixels are not the same in those axis. In the transversal axis the dimension of the pixel is 0.25 millimeters whereas in the longitudinal axis the dimension is 2 millimeters. The Z-axis that is the height of the protrusions is measured as the maximum value measured in the zone. The dimensions and the results are shown in the Figure 13 and the Table IV. These results show that the resolution of the system is set by the dimensions of the pixels, which is set by the sensors used and their acquisition frequency.

V. Conclusions

This paper proposes a new approach for surface inspection systems, based directly on the international standards the products must meet. This inspection system was developed, tested and validated using rails as an example, but it is also suitable for any other long product.

The proposed system is divided into two subsystems. One of them acquires profiles of the products in real-time using profilometers that are placed surrounding the products. The data acquired is aligned to the mathematical model of the product and their differences are used to produce differential topographic images of the surface of the products. This acquisition procedure was performed in 1.6 ms per profile in 99% of the tested cases. This speed allows the system to be installed in a real high-speed production line in which it can work in real-time conditions. This procedure is performed separately for each zone of the product in order to isolate the influence of dimensional problems in the zone in which they appear.

The produced images are processed using another subsystem to detect defects. The procedure used to detect defects is automatically configurable to avoid the cost of the common configuration process. The procedure was tested using a real set of samples reaching 60% of detection rate with only 8 erroneous detections per product. This low number of erroneous detection per product is also a requirement in a production line. The procedure uses directly the limits and rules of the international standards, which gives to the inspectors a way to discriminate if a surface annomaly meet the requirements needed or not. The system has been compared against two other industrial systems installed in the same production line giving better results.

The procedure was validated using a surface inspection rail pattern giving very good results. The validation of defect detection rate meets the ones obtained with the set of samples. The dimensional measurement validation also shows that the resolution is directly set by the acquisition frequency and the number of points acquired by the sensors. This resolution can be improved using another model of sensors which can acquire more points per profile working at a higher frequency.

The communication scheme proposed for the system allows any other machine from the factory to access to the results of the diagnosis and also to communicate with the system using message queues. This system has been installed in a ArcelorMittal factory as an industrial application giving the quality inspectors several ways to view the results of the diagnosis and measure the dimensions of the defects.

ACKNOWLEDGMENT

The authors would like to thank quality inspectors and personnel of ArcelorMittal for their help in the development of this research. This work has been partially funded by the project RTI2018-094849-B-I00 of the Spanish National Plan for Research, Development and Innovation and by the project FUO-269-19 funded by ArcelorMittal Research, Innovation and Investment S.L.

REFERENCES

[1] F. delaCalle Herrero, D. F. García, and R. Usamentiaga, "Rail surface inspection system using differential topographic images," in *2020 Industry Applications Society Annual Meeting, Detroit*. IEEE, 2020, pp. 1–8.

[2] W. Wei-han, "Product quality control and its applications in industry [j]," *Acta Simulata Systematica Sinica S*, vol. 1, 2001.

[3] E. N. Malamas, E. G. Petrakis, M. Zervakis, L. Petit, and J.-D. Legat, "A survey on industrial vision systems, applications and tools," *Image and Vision Computing*, vol. 21, no. 2, pp. 171 – 188, 2003.

[4] Z. Liu, H. Ukida, P. Ramuhalli, and K. Niel, *Integrated Imaging and Vision Techniques for Industrial Inspection*. Springer, 2015.

[5] F. M. Megahed and J. A. Camelio, "Real-time fault detection in manufacturing environments using face recognition techniques," *Journal of Intelligent Manufacturing*, vol. 23, no. 3, pp. 393–408, 2012.

[6] M. Patil, S. Verma, and J. Wakode, "A review on fabric defect detection techniques," *Int. Res. J. Eng. Technol*, vol. 4, no. 9, pp. 131–136, 2017.

[7] C. Jian, J. Gao, and Y. Ao, "Automatic surface defect detection for mobile phone screen glass based on machine vision," *Applied Soft Computing*, vol. 52, pp. 348–358, 2017.

[8] B. Zhang, W. Huang, J. Li, C. Zhao, S. Fan, J. Wu, and C. Liu, "Principles, developments and applications of computer vision for external quality inspection of fruits and vegetables: A review," *Food Research International*, vol. 62, pp. 326–343, 2014.

[9] E. Deutschl, C. Gasser, A. Niel, and J. Werschonig, "Defect detection on rail surfaces by a vision based system," in *IEEE Intelligent Vehicles Symposium, 2004*. IEEE, 2004, pp. 507–511.

[10] R. W. Conners, C. W. Mcmillin, K. Lin, and R. E. Vasquez-Espinosa, "Identifying and locating surface defects in wood: Part of an automated lumber processing system," *IEEE Transactions on Pattern Analysis and Machine Intelligence*, no. 6, pp. 573–583, 1983.

[11] J. L. Rose, M. J. Avioli, P. Mudge, and R. Sanderson, "Guided wave inspection potential of defects in rail," *Ndt & E International*, vol. 37, no. 2, pp. 153–161, 2004.

[12] Z. Xiong, Q. Li, Q. Mao, and Q. Zou, "A 3d laser profiling system for rail surface defect detection," *Sensors*, vol. 17, no. 8, p. 1791, 2017.

[13] O. Duran, K. Althoefer, and L. D. Seneviratne, "Automated pipe defect detection and categorization using camera/laser-based profiler and artificial neural network," *IEEE Transactions on Automation Science and Engineering*, vol. 4, no. 1, pp. 118–126, 2007.

[14] Y.-J. Jeon, D.-c. Choi, J. P. Yun, C. Park, and S. W. Kim, "Detection of scratch defects on slab surface," in *2011 11th International Conference on Control, Automation and Systems*. IEEE, 2011, pp. 1274–1278.

[15] F. G. Bulnes, D. F. García, F. J. De la Calle, R. Usamentiaga, and J. Molleda, "A non-invasive technique for online defect detection on steel strip surfaces," *Journal of Nondestructive Evaluation*, vol. 35, no. 4, p. 54, 2016.

[16] I. V. P. AG, "Isra vision parsytec ag, parallel system technology (parsytec)."

[17] R. J. Woodham, "Photometric method for determining surface orientation from multiple images," *Optical engineering*, vol. 19, no. 1, p. 191139, 1980.

[18] O. Ikeda and Y. Duan, "Color photometric stereo for albedo and shape reconstruction," in *2008 IEEE Workshop on Applications of Computer Vision*. IEEE, 2008, pp. 1–6.

[19] F. J. de la Calle Herrero, D. F. Garcia, and R. Usamentiaga, "Inspection system for rail surfaces using differential images," *IEEE Transactions on Industry Applications*, vol. 54, no. 5, pp. 4948–4957, 2018.

[20] L. Wang, K. Xu, and P. Zhou, "Online detection technique of 3d defects for steel strips based on photometric stereo," in *2016 Eighth International Conference on Measuring Technology and Mechatronics Automation (ICMTMA)*. IEEE, 2016, pp. 428–432.

[21] S. Seçil, K. Turgut, O. Parlaktuna, and M. Özkan, "3-d visualization system for geometric parts using a laser profile sensor and an industrial robot," in *2014 IEEE International Symposium on Robotics and Manufacturing Automation (ROMA)*. IEEE, 2014, pp. 160–165.

[22] Y. Santur, M. Karaköse, and E. Akin, "A new rail inspection method based on deep learning using laser cameras," in *2017 International Artificial Intelligence and Data Processing Symposium (IDAP)*. IEEE, 2017, pp. 1–6.

[23] Y. Qian, P. Cao, W. Yin, F. Dai, F. Hu, Z. Yan *et al.*, "Calculation method of surface shape feature of rice seed based on point cloud," *Computers and Electronics in Agriculture*, vol. 142, pp. 416–423, 2017.

[24] J. Hoła, Ł. Sadowski, J. Reiner, and S. Stach, "Usefulness of 3d surface roughness parameters for nondestructive evaluation of pull-off adhesion of concrete layers," *Construction and Building Materials*, vol. 84, pp. 111–120, 2015.

[25] J. Molleda, R. Usamentiaga, Á. F. Millara, D. F. García, P. Manso, C. M. Suárez, and I. García, "A profile measurement system for rail manufacturing using multiple laser range finders," in *2015 IEEE Industry Applications Society Annual Meeting*. IEEE, 2015, pp. 1–8.

[26] J. Molleda, R. Usamentiaga, D. F. García, and F. G. Bulnes, "Real-time flatness inspection of rolled products based on optical laser triangulation and three-dimensional surface reconstruction," *Journal of Electronic Imaging*, vol. 19, no. 3, p. 031206, 2010.

[27] M. Zhang, J. Wu, H. Lin, P. Yuan, and Y. Song, "The application of one-class classifier based on cnn in image defect detection," *Procedia computer science*, vol. 114, pp. 341–348, 2017.

[28] T. Wang, Y. Chen, M. Qiao, and H. Snoussi, "A fast and robust convolutional neural network-based defect detection model in product quality control," *The International Journal of Advanced Manufacturing Technology*, vol. 94, no. 9-12, pp. 3465–3471, 2018.

[29] X. Xu, Y. Lei, and F. Yang, "Railway subgrade defect automatic recognition method based on improved faster r-cnn," *Scientific Programming*, vol. 2018, 2018.

[30] G. Singh, G. Singh, and M. Kaur, "Fabric defect detection using series of image processing algorithm & ann operation," *Global Journal of Computers & Technology*, vol. 4, no. 2, pp. 225–229, 2016.

[31] "European standards bs en 13674-1:2011+a1:2017 railway applications. track. rail vignole railway rails 46 kg/m and above," 2017.

[32] F. J. de la Calle Herrero, D. F. Garcia, and R. Usamentiaga, "Generation of differential topographic images for surface inspection of long products," *Journal of Real-Time Image Processing*, pp. 1–14, 2019.

[33] F. delaCalle Herrero, D. F. García, and R. Usamentiaga, "Surface defect system for long product manufacturing using differential topographic images," *Sensors*, vol. 20, no. 7, p. 2142, 2020.

[34] R. O. Duda, P. E. Hart, and D. G. Stork, *Pattern classification*. John Wiley & Sons, 2012.

[35] D. ping Tian *et al.*, "A review on image feature extraction and representation techniques," *International Journal of Multimedia and Ubiquitous Engineering*, vol. 8, no. 4, pp. 385–396, 2013.